Non-equilibrium and residual memory in momentum space of fragmenting sources in central heavy-ion collisions

Jun Su[1,2] and Feng-Shou Zhang[1,2,3,*]

[1]*The Key Laboratory of Beam Technology and Material Modification of Ministry of Education, College of Nuclear Science and Technology, Beijing Normal University, Beijing 100875, China*

[2]*Beijing Radiation Center, Beijing 100875, China*

[3]*Center of Theoretical Nuclear Physics, National Laboratory of Heavy Ion Accelerator of Lanzhou, Lanzhou 730000, China*

(Received 15 November 2012; published 30 January 2013)

The non-equilibrium in momentum space of fragmenting sources in central heavy-ion collisions at Fermi energy is reproduced by partly compensating for the fermionic feature in the isospin-dependent quantum molecular dynamics model. A memory loss ratio is defined to investigate the degree of entrance channel memory loss. The incomplete memory loss and the linear correlation between the memory loss ratio and the normalized radial flow energy are found both from experimental data and calculations. The residual memory indicates that the global equilibrium is not achieved in central collisions. The local equilibrium is achieved only in a very small central region of the fragmenting source. Both the asymmetry distribution of the expansive flow and the deformation of the fragmenting source are the consequences of the residual memory. A method to extract the transversal-to-longitudinal axis ratio of the expanding fragmenting source is suggested.

DOI: 10.1103/PhysRevC.87.017602 PACS number(s): 25.70.Pq, 25.75.Ld

During the last 20 years, the studies of heavy-ion collisions (HICs) were motivated by purposes to obtain information on multifragmentation and its relationship to the liquid-gas-type phase transition [1,2]. Experimental signals of phase transitions have been observed by several experimental groups [3–7]. Many theoretical efforts to find the signatures of phase transitions in HICs started a few years ago [8–12]. Based on different statistical ensembles, statistical approaches have been adopted to describe the general features of the multifragmentation [13–18]. However, in understanding the phase transitions in HICs, it is still a challenge to develop the statistical description of the open transient finite systems [19].

Indeed, the equilibrium hypothesis, used in the construction of statistical ensembles, is not guaranteed *a priori* in HICs. Some evidence of non-equilibrium with respect to isospin degree of freedom has been found [20–24]. In 1988, Bauer predicted that the degree of stopping could be the sensitive observable to check the nuclear equilibration [25]. Recently, systematic experimental measurements in the wide energy range from Fermi energy to GeV/nucleon have supported the prediction of incomplete stopping and indicated that the global equilibrium was not achieved even for the most central collisions and for the most massive systems [26–28]. Based on different dynamical theories, analyses of the stopping data have been presented [29–31]. The non-equilibrium statistical mechanics [32] seems to be required to investigate the evolving nuclear systems in HICs. Therefore, investigations of the residual memory could be important.

The effects of the transparency and entrance channel memory could influence the spherical symmetry of the expanding system [33]. The radial flow and the side flow, reflecting the character of the early stage of the collisions, have been found to be correlated to the global stopping in central collisions at energies above 150 MeV/nucleon [27,34]. However, data measured at energies below 150 MeV/nucleon do not continue the same linear correlation [35]. The prolate deformation of the emitting source has been indicated from the angular anisotropy of the fragment sizes and the kinetic energies in central HICs at intermediate energies [36,37]. Since the radial flow can transform the spatial correlations into correlations in momentum space [37], the spherical symmetry of the radial flow has to be studied in detail. Detailed information on the expansion dynamics is required to find the dynamical origin of the source deformation.

In this Brief Report, the global stopping and the radial flow energy in central HICs at Fermi energy are investigated by the isospin-dependent quantum molecular dynamics (IQMD) model in combination with the statistical decay code GEMINI. A memory loss ratio is defined to quantify the residual memory and the deviation from the equilibrium. The residual memory is probed both from experimental data and calculations.

In the IQMD model [38], both soft (S) and hard (H) equations of state (EOS) [39] are applied. The nucleon-nucleon (NN) cross sections are modified by the in-medium factor of $1 - 0.2\rho/\rho_0$ [40]. To compensate for the fermionic feature the method of the phase-space density constraint in the constrained molecular dynamics model [41] is applied. For the comparison of the calculations with the experimental data, it is necessary to include the decays of the prefragments by the statistical code GEMINI [42].

Actually, the NN cross section is reduced to an effective cross section by including the Pauli blocking. Whenever a collision occurs, the phase space around the final states of the scattering partners must satisfy the Pauli principle. In the usual Pauli-blocking method (named PAULI1 in the following), the phase-space density f_i' at the final states is measured and interpreted as a blocking probability. Thus, the collision is only allowed with a probability of $(1 - f_1')(1 - f_2')$. The Pauli-

*Corresponding author: fszhang@bnu.edu.cn

 ©2013 American Physical Society

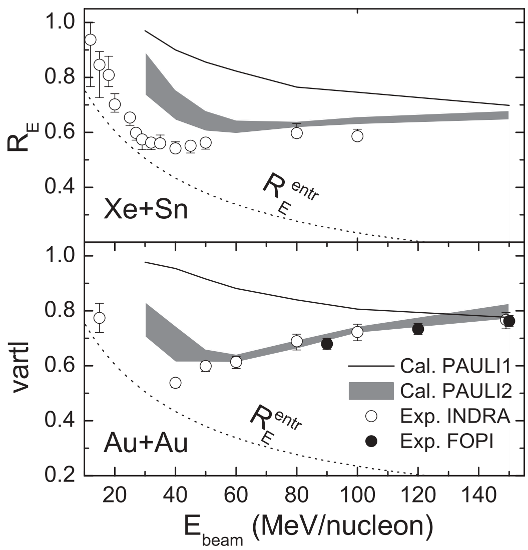

FIG. 1. Nuclear stopping quantified both by R_E in central Xe + Sn collisions and *vartl* in central Au + Au collisions. The isotropy ratio $R_E^{\rm entr}$ in the entrance channels is shown by dotted lines. Experimental data are taken from Refs. [27,28,35].

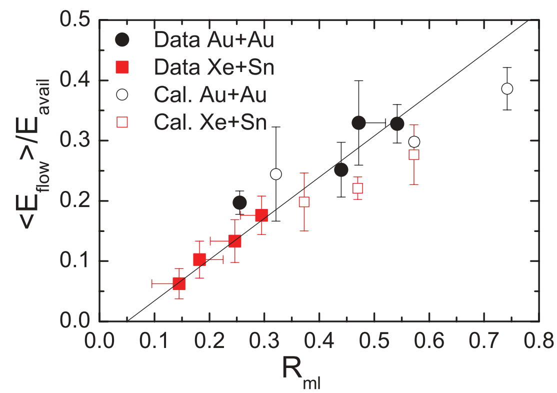

FIG. 2. (Color online) Correlation between the normalized flow energy $E_{\rm flow}/E_{\rm avail}$ and the memory loss ratio $R_{\rm ml}$. The solid line is for guiding the eyes. The calculated flow energies are extracted from the mass-dependent kinetic energy of Li fragments. The experimental data of flow energies are taken form Refs. [7,36]. The lack of error bars for experimental data means that the errors cannot be identified from the published experimental data.

blocking method related to the phase-space density constraint is used in this work (named PAULI2 in the following). In fact the phase-space occupation $\overline{f}_i$ is calculated by performing the integration on a hypercube of volume h^3 in the phase space centered around the final states (see Eq. (16) in Ref. [41]). The collision is accepted if the phase-space occupations $\overline{f}_i$ at the final state are both less than 1.

To quantify the degree of stopping, one adopts the ratio of transverse to parallel quantities, such as *vartl* [27] and R_E [28]. The excitation functions of R_E for central Xe + Sn collisions ($b < 1.6$ fm) and *vartl* for central Au + Au collisions ($b < 2.0$ fm) at the beam energy from 10 to 150 MeV/nucleon are shown in Fig. 1. The isotropy ratios $R_E^{\rm entr}$ in the entrance channels are also shown in the figure (dotted lines). The experimental data of R_E (circles in top panel) are characterized by the minimum near the Fermi energy with raises above and below. The obtained data of *vartl* (circles in bottom panel) also follow the same general trend. However the exact position of the minimum is not shown due to the lack of data near the Fermi energy. Two Pauli-blocking methods are compared. The results by PAULI1 (solid lines) show a monotonic decrease with increasing incident energy. The results by PAULI2 are shown by the gray area with the upper edge for H EOS and the lower edge for S EOS. They reproduce the general trend of the data, though the positions of the minimums are both lager than the Fermi energy. A comparison of the upper and lower edges of the gray area shows that the global stopping depends on the EOS, especially at low energies. The S EOS is more effective than the H EOS. In the following calculations, we adopt the S EOS and the PAULI2 method.

The incomplete stopping indicates that the fireballs from the central collisions do not lose all memories from the entrance channels. The values of *vartl* and R_E are compared to the isotropy ratio $R_E^{\rm entr}$ in the entrance channels (shown by dotted lines in Fig. 1). Below the Fermi energy the experimental points are close to the dotted lines, indicating that the memories are almost kept due to the lack of NN collisions. For the incident energies higher than the Fermi energy, the experimental points are far from the dotted lines. This reflects the fact of the memories' loss in the momentum space during the collisions. The memory loss ratio $R_{\rm ml}$ is defined to quantify the memory loss

$$R_{\rm ml} = \frac{R_E - R_E^{\rm entr}}{1 - R_E^{\rm entr}}. \tag{1}$$

If the fireballs from the central collisions lost all of the entrance channel memories, the value of $R_{\rm ml}$ is expected to be 1. On the contrary, the value 0 reflects that the fireballs keep all the entrance channel memories.

Figure 2 presents the radial flow energy normalized to the total available kinetic energy in the center of mass $E_{\rm flow}/E_{\rm avail}$ as a function of the memory loss ratio $R_{\rm ml}$. The radial flow energies of the experimental data are extracted from statistical model fitting to the experimental observables, such as the fragment transversal energies [7,36]. The method adopted here to extract the flow energies is the linear fit of the relationships between the calculated kinetic energy and mass of the Li fragments. It is shown that both the experimental data and the calculations show a positive correlation between the normalized flow energy and the memory loss ratio. The line in the figure guides this correlation. For collisions at incident energy larger than 150 MeV/nucleon, the isotropy ratio $R_E^{\rm entr}$ in the entrance channels is very small. The memory loss ratio $R_{\rm ml}$ approximately equals the isotropy ratio R_E, which is used to quantify the global stopping. Therefore, the normalized flow energy is correlated to the stopping in central collisions at energies above 150 MeV/nucleon, just as reported in Ref. [34].

To analyze the dynamical origin of the correlation between the flow energy and the memory loss, we investigate the time evolution of several observables. Figure 3(a) shows the time evolutions of the potential energy, the transversal flow energy,

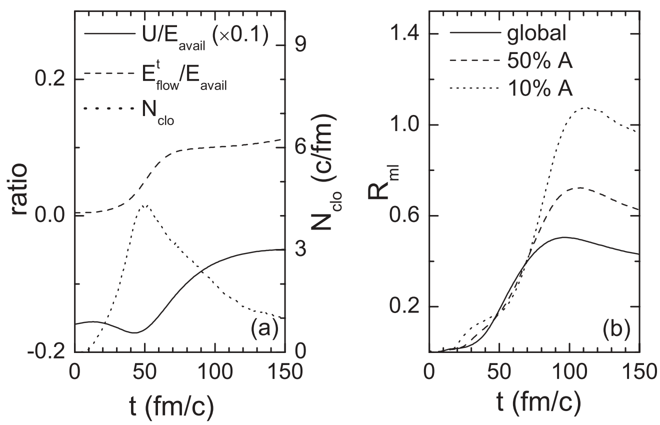

FIG. 3. (a) Time evolutions of the potential energy, the transversal flow energy, and the number of NN collisions in central Au + Au collisions at 60 MeV/nucleon. (b) Time evolutions of the memory loss ratio R_{ml} for the same reaction system. The solid line represents the global one. The dashed line and dotted line represent the local ones for the central region including 50% and 10% of the nucleons, respectively.

and the number of NN collisions in central Au + Au collisions at 60 MeV/nucleon. The evolution of the potential energy can describe the global compression and expansion. It is shown that the strongest compression occurs at 45 fm/c, when the potential energy reaches the minimum value. Since the nuclear system is compressed in the longitudinal direction, it is NN collisions that may make the longitudinal compression and expansion transfer to the radial direction. The transversal flow energy increases visibly at the time from period 30 to 70 fm/c, when the number of NN collisions is large. Meanwhile, the NN collisions are responsible for the memory loss.

Figure 3(b) shows the time evolution of the memory loss ratio R_{ml}. The solid line represents the global one. The dashed line and the dotted line represent the local ones for the central region including 50% and 10% of the nucleons, respectively. It is shown that the memory loss depends strongly on the considered location of the colliding system. The nucleons from the peripheral region keep more memories than the central ones. Since the global R_{ml} does not reach the value of 1, the global equilibrium is not achieved. The residual memory of the half nucleons in the central region opposes the hypothesis that an equilibrated fragmenting source is formed in HICs. Only a small central region, about 10% of the central nucleons, lose all memories.

The motion of the fragments in central collisions is a combination of the thermal motion, the Fermi motion, the radial flow, and the Coulomb repulsive motion, where the first two are isotropic. Thus the residual memory of the entrance channels is manifested as the asymmetry distribution of the radial flow and the Coulomb repulsive motion. Adopting a prolate shape in coordinate space and a proportional relation $\mathbf{p}(\mathbf{r}) = r^{\alpha} p_0 \frac{\mathbf{r}}{r}$ [13,36], it can be derived by integration that the shape of the collective expansion is also prolate. One obtains flow energy as a function of the polar angle

$$E_{\mathrm{flow}}(\theta) \propto \left(\frac{1}{\mathcal{R}^2}\sin^2\theta + \cos^2\theta\right)^{-\alpha}, \qquad (2)$$

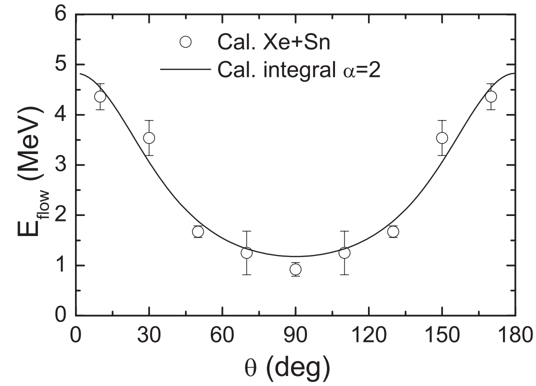

FIG. 4. Calculated flow energy as a function of the polar angle in central Xe + Sn collisions at 50 MeV/nucleon.

where $\mathcal{R}$ is the transversal-to-longitudinal axis ratio of the fragmenting source in coordinate space. The value of α depends on the expansion dynamics. For the self-similar expansion, the value of α is equal to 1. However, as shown in Fig. 3(a), the radial expansion velocity increases during the expansion. The value of α for the fragmenting source will be larger than 1. The value 2 for α is adopted in this work, the same as in Ref. [36].

To demonstrate, the polar-angle-dependent flow energies for Xe + Sn collisions at 50 MeV/nucleon are shown in Fig. 4. The values of the flow energy at the polar angle θ and $\pi - \theta$ are extracted simultaneously using the symmetry of the distribution. The contribution to the error bars of the calculations comes from the fits of the kinetic energies. One can see that the longitudinal flow energy is larger than the transversal flow energy. When fitting the discrete points by the function (2) with $\alpha = 2$ and $\mathcal{R} = 0.68$, a good agreement is obtained. The transversal-to-longitudinal axis ratio of the fragmenting source can be extracted from the flow energies at forward and sideward angles. The results for Xe + Sn and Au + Au at different energies are shown in Table I. The values extracted by other methods are shown as well. A similar deformation is found.

In conclusion, for central collisions in the Fermi energy range, the entrance channel memory in momentum space is not completely lost. For the memory loss, the global equilibrium is not achieved. When reproducing this non-equilibrium in the dynamical models such as IQMD, it is significant to describe accurately the Pauli exclusion principal. The memory loss ratio shows a strong correlation to the radial flow energy normalized to the total available kinetic energy in the center of mass. Some analyses of the dynamical origin of this correlation are presented. Based on our calculations, we cannot draw a conclusion that an equilibrated fragmenting source is formed in HICs. The local equilibrium is achieved only in a very small central region of the fragmenting source. The residual memory of the entrance channel is manifested as the asymmetry distribution of the radial flow. The asymmetry expansion is the dynamical origin of the source deformation. It is suggested that the transversal-to-longitudinal axis ratio of the fragmenting source could be extracted from the flow energies at forward and sideward angles.

TABLE I. Transversal-to-longitudinal axis ratio $\mathcal{R}$ of the expanding fragmenting source at freeze-out.

System E_{beam} (MeV/nucleon)	Xe + Sn 50	Au + Au 60	Au + Au 80	Au + Au 100
This work	0.68 ± 0.20	0.72 ± 0.14	0.67 ± 0.23	0.69 ± 0.07
Ref. [36]	0.70	0.70	0.70	0.76
Ref. [37]	0.7	–	–	–

This work was supported by the National Natural Science Foundation of China under Grant Nos. 11025524 and 11161130520, and the National Basic Research Program of China under Grant No. 2010CB832903.

[1] *Dynamics and Thermodynamics with Nucleonic Degrees of Freedom*, edited by P. Chomaz, F. Gulminelli, W. Trautmann, and S. J. Yennello (Springer, New York, 2006).
[2] B. Borderie and M. F. Rivet, Prog. Part. Nucl. Phys. **61**, 551 (2008).
[3] M. L. Gilkes *et al.* (EOS Collaboration), Phys. Rev. Lett. **73**, 1590 (1994).
[4] J. Pochodzalla *et al.*, Phys. Rev. Lett. **75**, 1040 (1995).
[5] M. D'Agostino *et al.*, Phys. Lett. B **473**, 219 (2000).
[6] E. Bonnet *et al.* (INDRA ALADIN Collaborations), Phys. Rev. Lett. **103**, 072701 (2009).
[7] B. Borderie *et al.*, Nucl. Phys. A **734**, 495 (2004).
[8] P. Borrmann, O. Mülken, and J. Harting, Phys. Rev. Lett. **84**, 3511 (2000).
[9] P. Chomaz, V. Duflot, and F. Gulminelli, Phys. Rev. Lett. **85**, 3587 (2000).
[10] A. H. Raduta and A. R. Raduta, Phys. Rev. Lett. **87**, 202701 (2001).
[11] J. B. Natowitz *et al.*, Phys. Rev. Lett. **89**, 212701 (2002).
[12] L. G. Moretto *et al.*, Phys. Rev. Lett. **94**, 202701 (2005).
[13] J. P. Bondorf, S. I. A. Garpman, and J. Zimanyi, Nucl. Phys. A **296**, 320 (1978).
[14] J. Randrup and S. E. Koonin, Nucl. Phys. A **356**, 223 (1981).
[15] D. H. E. Gross *et al.*, Z. Phys. A **309**, 41 (1982).
[16] D. Durand, Nucl. Phys. A **541**, 266 (1992).
[17] Al. H. Raduta and Ad. R. Raduta, Phys. Rev. C **55**, 1344 (1997).
[18] W. P. Tan *et al.*, Phys. Rev. C **68**, 034609 (2003).
[19] P. Chomaz and F. Gulminelli, Eur. Phys. J. A **30**, 317 (2006).
[20] F. Rami *et al.* (FOPI Collaboration), Phys. Rev. Lett. **84**, 1120 (2000).
[21] Q. F. Li and Z. X. Li, Phys. Rev. C **64**, 064612 (2001).
[22] A. L. Keksis *et al.*, Phys. Rev. C **81**, 054602 (2010).
[23] Z. Y. Sun *et al.*, Phys. Rev. C **82**, 051603 (2010).
[24] S. J. Yennello *et al.*, Phys. Lett. B **321**, 15 (1994).
[25] W. Bauer, Phys. Rev. Lett. **61**, 2534 (1988).
[26] B. Hong *et al.*, Phys. Rev. C **66**, 034901 (2002).
[27] W. Reisdorf *et al.* (FOPI Collaboration), Phys. Rev. Lett. **92**, 232301 (2004).
[28] G. Lehaut *et al.* (INDRA ALADIN Collaborations), Phys. Rev. Lett. **104**, 232701 (2010).
[29] T. Gaitanos *et al.*, Phys. Lett. B **609**, 241 (2005).
[30] Y. X. Zhang, Z. X. Li, and P. Danielewicz, Phys. Rev. C **75**, 034615 (2007).
[31] G. Q. Zhang *et al.*, Phys. Rev. C **84**, 034612 (2011).
[32] R. Kubo, M. Toda, and N. Hashitsume, *Statistical Physics II, Nonequilibrium Statistical Mechanics*, Springer Ser. Solid-State Sci., Vol. 31 (Springer, Berlin, Heidelberg, New York, 1978).
[33] G. Stoicea *et al.* (FOPI Collaboration), Phys. Rev. Lett. **92**, 072303 (2004).
[34] F. Fu *et al.*, Phys. Lett. B **666**, 359 (2008).
[35] A. Andronic *et al.*, Eur. Phys. J. A **30**, 31 (2006).
[36] A. Le Fèvre *et al.* (INDRA ALADIN Collaborations), Nucl. Phys. A **735**, 219 (2004).
[37] A. Le Fèvre *et al.* (INDRA ALADIN Collaborations), Phys. Lett. B **659**, 807 (2008).
[38] C. Hartnack *et al.*, Nucl. Phys. A **495**, 303 (1989).
[39] G. F. Bertsch and S. Das Gupta, Phys. Rep. **160**, 189 (1988).
[40] G. D. Westfall *et al.*, Phys. Rev. Lett. **71**, 1986 (1993).
[41] M. Papa, T. Maruyama, and A. Bonasera, Phys. Rev. C **64**, 024612 (2001).
[42] R. J. Charity *et al.*, Nucl. Phys. A **483**, 371 (1988).